P2-25

Effect of N_2, Ne and Ar seeding on Alcator C-Mod H-mode confinement

M. L. Reinke[a], J. W. Hughes[a], A. Loarte[b], D. Brunner[a], I. H. Hutchinson[a],

B. LaBombard[a], J. Payne[a], and J. L. Terry[a]

[a]*MIT Plasma Science and Fusion Center, 175 Albany St., Cambridge MA 02139*

[b]*ITER Organization, Route de Vinon CS 90046, 13067 Saint Paul lez Durance Cedex, France*

The mitigation of divertor heat fluxes is an active topic of investigation on existing tokamaks. One approach uses radiation, both inside and outside the last closed flux surface (LCFS), to convert plasma thermal energy, usually directed towards dedicated plasma facing components, to soft x-ray and ultraviolet radiation, spread over a much larger surface area. Recent enhanced D-α H-mode experiments on Alcator C-Mod varied the ICRF input power and radiative power losses via impurity seeding to demonstrate that normalized energy confinement depends strongly on the difference between input power and the radiated power inside the LCFS. These investigations also show that when seeded with either Ne or N_2, a factor of two and higher reduction in outer divertor heat flux is achieved while maintaining $H_{98,y2} \sim 1.0$. Conversely, when seeding with Ar, confinement is limited to $H_{98,y2} \sim 0.8$ for a similar level of exhaust power.

PACS: 52.55.Fa, 52.55.Rk, 52.25.Vy, 28.52.Cx

JNM keywords: P0600

PSI-19 keywords: Alcator C-Mod, Energy Confinement, Impurity, Radiation, Power Balance

*Corresponding author address: NW17-225, 175 Albany St, Cambridge, MA, 02141

*Corresponding and presenting author E-mail: mlreinke@psfc.mit.edu

Presenting author: M. L. Reinke

I. INTRODUCTION

The removal of core heat exhaust has been identified as one of the primary challenges facing the extrapolation of current tokamaks designs to demonstration reactors [1]. To reduce the heat flux to plasma facing components (PFCs) to the ~10 MW/m^2 level, two approaches are being actively investigated. The first is to spread the conducted power over a wider area, either through magnetic flux expansion or bringing the same SOL power to PFCs at larger major radii [2]. The second, addressed here, seeks to reduce the amount of power reaching PFCs by using impurities inside and outside the LCFS to convert plasma thermal energy to isotropic ultraviolet and soft x-ray radiation. This technique has been investigated on a number of tokamaks in both type-I and type-III (edge-localized mode) ELM regimes, though maintaining high normalized confinement has not always been demonstrated [3-7]. The present work reports the results of experiments on enhanced D-α (EDA) H-mode plasmas [8] in Alcator C-Mod where the impact to the energy confinement from varying amounts of seeded radiation loss and ICRF input power were investigated. The experimental energy confinement time, $\tau_E = W_{TH}/(P_{IN}-dW_{TH}/dt)$, where W_{TH} is the stored energy calculated from the EFIT pressure profile, is normalized to the ITER98(y,2) scaling and referred to as the H-factor or H_{98}. These experiments demonstrate, in a fixed configuration, $H_{98} \sim 1.0$ operations with a 50% or more reduction in the power to the outer divertor when N_2 or Ne seeding is utilized. Seeding with Ar resulted in similar reductions in divertor heat loading but core confinement drops to $H_{98} < 0.8$. Section II of this paper describes the diagnostic tools used for these studies, Section III presents the effect of seeded impurity radiation on confinement and Section IV presents the reduction in divertor exhaust power and discusses the implication of these results.

II. DESCRIPTION OF EXPERIMENTS

These investigations were completed for EDA H-modes, a steady-state H-mode regime commonly utilized on Alcator C-Mod, where the pedestal gradients are continuously relaxed via the so-called quasi-coherent mode [8] rather than by discrete type-I ELMs typical in most tokamak H-mode regimes. Line-integrated radiation is measured using an absolutely calibrated resistive bolometer array on the low-field side (LFS) midplane and Abel-inverted to find the radial emissivity profile [9]. An estimate of the global radiated power is made using a wide-angle bolometer that includes the core and a portion of the divertor radiation. This unit is calibrated by seeding an ICRF-heated plasma to radiative collapse and assuming the signal measured to be equal to the input power. Both these units are sensitive the power deposited by neutrals, but this is assumed to be small compared to the radiative losses due to heavy impurity seeding. The heat flux in the divertor is calculated using an infrared thermography diagnostic described in more detail in [10]. Time evolving profiles of surface temperature constrain a 2D heat-transport model to calculate the surface heat-flux profile at the outer divertor which is then integrated over the divertor surface, assumming toroidal symmetry to calculate the total power to the outer divertor, $P_{O\text{-}DIV}$. Thomson scattering with ~1 mm resolution is used to measure the electron temperature and density profiles in the pedestal region [11].

To test the effect of radiative power loss on confinement a single discharge was repeated adjusting input ICRF power level as well as the type and amount of impurity seeding. N_2, Ne and Ar seeded H-modes were analyzed along with unseeded H-modes, with all plasmas having varying amounts of radiation due to intrinsic Mo and B. The extrinsic impurity seeding was done through a main-chamber piezoelectric gas valve with the pressure of the puff varied to change the impurity fraction. All plasmas had I_p ~0.8 MA, B_t ~ 5.4 T and relatively weak shaping (δ_{upper} ~ 0.2, δ_{lower} ~ 0.5 and κ ~ 1.5). The line-averaged density varied slightly depending on confinement but was nominally 3.0×10^{20} m^{-3} or approximately $\langle n_e \rangle / n_G \sim 0.5$. The L-H threshold power was measured using slow

ICRF power ramps, but showed significant variation between different run days with $P_{L\text{-}H} \sim 1.75$ +/- 0.35 [MW], between 1.0-1.5 the accepted scaling [12]. Figure 1 shows the time history of a typical N_2, Ne and Ar seeded discharge. Gas puffs were started before the L-H transition and recycling of Ar and Ne allowed for slowly evolving radiation during the 4-5 MW ICRF power scan. Additional Ne puffs were required at the highest radiation levels, while for N_2, a steady-state puff was required to combat the drop in recycling. Total input power, $P_{IN}=P_{OH}+P_{ICRF}$, shown in Figure 1c, is calculated assuming 90% absorption of the ICRF power leaving the antenna. Figure 1d shows the radiated power from the two different measurements discussed earlier. The power loss inside the last closed flux-surface (LCFS), $P_{RAD,LCFS}$ is calculated by assuming the radial emissivity profile is flux-surface symmetric and integrating over the plasma volume and is represented by the dashed lines. Emissivity profiles remain hollow for all plasmas, although the edge/core ratio is lower for Ar seeding then for Ne or N_2. The solid lines show the time evolution of the estimated global radiated power and comparisons to $P_{RAD,LCFS}$ indicate a higher fraction of divertor radiation as the Z of of the seeded impurity, Z_{SEED}, is decreased. Figure 1e demonstrates the H_{98}~1.0 operations, although for this particular Ar seeding level it is reached transiently with the rise in radiated power after t~1.0 s correlated with a drop in H-factor. The power to the outer divertor is shown in Figure 1f where the Ar-seeded plasma, with the highest $P_{RAD,LCFS}$, also has the highest $P_{O\text{-}DIV}$, while the N_2-seeded plasma, with the lowest $P_{RAD,LCFS}$ has the lowest $P_{O\text{-}DIV}$. This also implies the presence of enhanced divertor radiation as Z_{SEED} is decreased, although $P_{RAD,DIV}$ is currently not directly measured.

III. EFFECT OF RADIATION ON CONFINEMENT

Thirty discharges were analyzed, using time-averaged segments of 30 ms duration, each having quasi-steady input power and radiation. The entire dataset is shown in Figure 2 where H_{98} is plotted against $P_{SOL}=P_{IN}-P_{RAD,LCFS}$, indicating that for a given value of P_{SOL} there is a maximum achievable

H_{98} that increases as power through the LCFS is raised. At higher P_{SOL} values, normalized confinement appears to drop, correlated with significant increases in edge neutral density, in a manner that is consistent with prior experience with D_2 gas puffing into EDA H-modes [13]. In order to account for background neutral pressure, p_{WALL} variation due to PFC outgassing, an average over the LFS midplane Ly-α brightness profile is is used as a proxy since the two are expected to be tightly correlated. In Figure 2, different ranges of Ly-α brightness are isolated and it is clear that at fixed P_{SOL}, increased edge neutral pressure is correlated with reduced confinement.

To study the Z_{SEED} and P_{SOL} dependance of H_{98}, the dataset is truncated to where the Ly-α brightness is less than 45 kW/m^2 which corresponds to p_{WALL} below 0.2 mTorr. The effect of different impurity species is shown in Figure 3a with H_{98} again plotted against P_{SOL}, this time differentiated by impurity species. At low levels of seeding, where P_{SOL} is much greater than that at the L-H threshold, all cases overlap and show an increase in H_{98} with P_{SOL}. This trend appears consistent with core profile stiffness arguments as the height of of the electron temperature pedestal, $T_{e,ped}$, is correlated with the normalized confinement as shown in Figure 3b. A systematic difference in confinement is observable at low $T_{e,ped}$ for different impurities seeding cases. Core electron temperature profiles need to be examined in more detail to see if the gradient scale length is affect ed by enhanced core power loss from higher-Z impurities. As P_{SOL} approaches the L/H threshold power, differences in H_{98} are also observed between different impurities in Figure 3a. The low P_{SOL} unseeded cases consist mainly of low P_{IN}, low P_{RAD} data while the low P_{SOL} Ar cases are mostly high P_{IN}, high P_{RAD} points, suggesting a hysteresis [14] as the L-H threshold is approached with heavy seeding.

IV. DISCUSSION

The results from Section III illustrate that, regardless of the variety of power sources and sinks, normalized confinement depends primarily on the net power through the plasma edge. In this context, applying techniques which seek to remove heat from the plasma outside of the core but inside of the LCFS, the so-called radiative mantle, provides no benefit if P_{IN} is near the $P_{L\text{-}H}$. Such a trend also sets a clear mission for radiative divertor scenarios since the L-H threshold power or greater will need to be deposited into the SOL and a large fraction not allowed to reach the PFCs. Converting this power into radiation outside the LCFS must be done with minimal increase in core radiation which suggests low-Z impurities will be the most efficient as shown previously on Alcator C-Mod [15]. This can now be shown more conclusively by comparing H_{98} to power to the outer divertor as measured with new IR thermography diagnostics discussed in Section II. As shown in Figure 4a., these experiments demonstrate nearly a factor of two reduction in $P_{O\text{-}DIV}$ with H_{98}~1.0 when using Ne seeding. Extrapolating the trends to P_{ODIV}=0 (i.e. detachement) for both Ne and Ar seeding would result in L-mode levels of energy confinement, consistent with earlier experiments [15]. Although the C-Mod thermography data for N_2-seeded plasmas is limited to a few time slices, a x5 reduction of $P_{O\text{-}DIV}$ is observed while still maintaining H_{98}~1.0 also in agreement with past results. When $P_{O\text{-}DIV}$ is normalized to the input power as shown in Figure 4b, the Ne and N_2 seeded plasmas are able to reach the desired outer divertor loading condition for ITER [1]. To reduce $P_{O\text{-}DIV}/P_{IN}$ to such a level when seeding with higher-Z impurities or operating without seeding results in much lower, $H_{98} \sim 0.8$, confinement.

These results show that in an EDA H-mode configuration, an operating space in Z_{SEED} and n_z exists where $H_{98} \geq 1.0$ operations are possible with reduced divertor heat flux. To apply these results to other C-Mod plasmas and other devices or confinement regimes requires understanding of what determines the boundaries of this space. The electron temperature-dependent radiation physics certainly plays a primary role but impurity transport in the pedestal and divertor can also expected to be important. The observed deterioration of confinement with increasing Mo or Ar levels is expected from a pedestal height that increases with edge conducted power since a substantial amount of the radiation is well inside the LCFS. As Z_{SEED} decreases, the radiation layer moves towards lower temperatures approaching the the plasma edge and divertor. The data shown in Figure 3a cannot make a distinction between the LCFS and the top of the pedestal and it is unclear if there exists a region between the two where radiation will not effect the height of the pedestal. Additionally, we expect some poloidal variation of the edge radiation layer in the vicinity of the x-point which will require a more comprehensive bolometer diagnostic.

ACKNOWLEDGEMENTS

The authors would like to thank S. M. Wolfe for useful discussions and to the entire C-Mod team for expert operation of the tokamak. This work is supported by DOE contract number DE-FC0299ER54512.

REFERENCES:

[1] A. Loarte, *et al*. Nucl. Fusion. **47** (2007) S203

[2] M. Kotschenreuther, *et al*. Phys. of Plasmas. **14** (2007) 072502

[3] J.A. Goetz, *et al*. Phys. of Plasmas. **6** (1999) 1899

[4] P. Monier-Garbet, *et al*. Nucl. Fusion. **45** (2005) 1404

[5] T.W. Petrie, *et al.* J. Nucl. Mater. **363-365** (2007) 416

[6] N. Asakura, *et al*. Nucl. Fusion. **49** (2009) 115010

[7] O. Gruber, *et al*. Nucl. Fusion. **49** (2009) 115014

[8] M. Greenwald, *et al*. Fusion Sci. Technol. **51** (2007) 266

[9] M.L. Reinke, *et al*. Rev. Sci. Instrum. **79** (2008) 10F306

[10] J.L. Terry, *et al*. Submitted to Rev. Sci. Insturm. (2010)

[11] J.W. Hughes, *et al*. Rev. Sci. Instrum. **72**(2001) 1107

[12] Y. Martin, *et al*. Journal of Physics: Conference Series **123** (2008) 012033

[13] J.W. Hughes, *et al*. Nucl. Fusion. **47** (2007) 1057

[14] A.E. Hubbard, *et al*. Plasma Phys. Control. Fusion. **44** (2002) A359

[15] B. Lipschultz, *et al*. J. Nucl. Mater. **241-243** (1997) 771

FIGURE 1: Time history of a typical nitrogen (green), neon (blue) and argon (red) seeded EDA H-mode used in these experiments. Impurity seeding (a) begins prior to application of ICRF heating (c) which induces the L-H transition as evident in the density (a) and temperature (b) traces. Radiated power (d) inside the LCFS (dashed) and the estimated global P_{RAD} (solid) increase as well. Steady confinement (e) of H_{98}~1.0 is reached with Ne and N_2 seeding with low power to outer divertor (f) measured using IR thermography.

FIGURE 2: Correlation of normalized confinement, H_{98}, with power to the scrape-off layer, P_{SOL}. Neon seeded shots (open symbols) are distinguished by brightness of edge viewing Lyman-α, correlated to edge neutral pressure. Including remaining data (small black circles) shows an empirical limit to the achievable H_{98} for a given P_{SOL}

FIGURE 3: (a) Correlation of H_{98} with P_{SOL} for different impurity seeding. Above the L-H threshold power the confinement scales with P_{SOL} regardless of the seeding species. This trend is consistent with core profile stiffness (b) as the confinement is tightly coupled to the height of the electron temperature pedestal

FIGURE 4: (a) When using Ne and N_2 seeding, good energy confinement (H_{98} ~ 1.0) be maintained as power to the outer divertor, $P_{O\text{-}DIV}$, is reduced by ~50% in contrast to Ar which results in H98 < 0.9. (b) Normalized to input power, the outer divertor loading approaches levels desired by ITER .

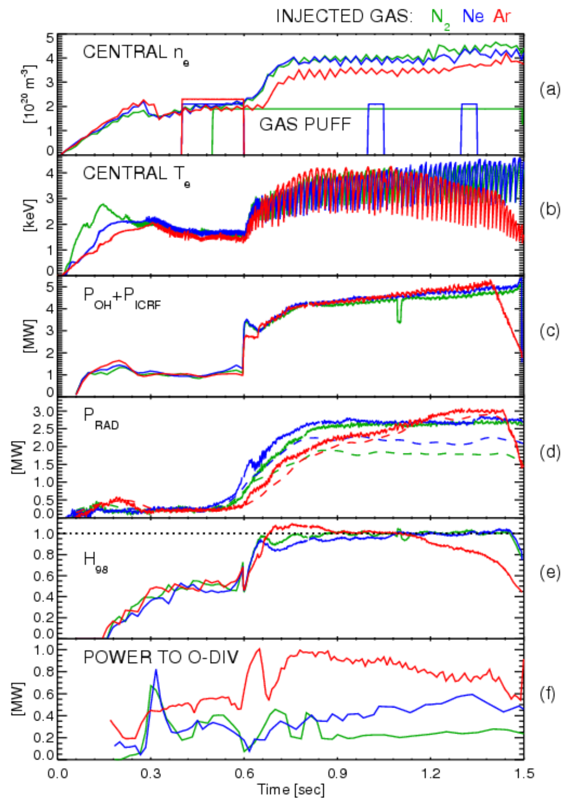

INJECTED GAS: N2 Ne Ar
CENTRAL ne
[10^20 m^-3]
GAS PUFF
(a)
CENTRAL Te
[keV]
(b)
POH+PICRF
[MW]
(c)
PRAD
[MW]
(d)
H98
(e)
POWER TO O-DIV
[MW]
(f)
Time [sec]

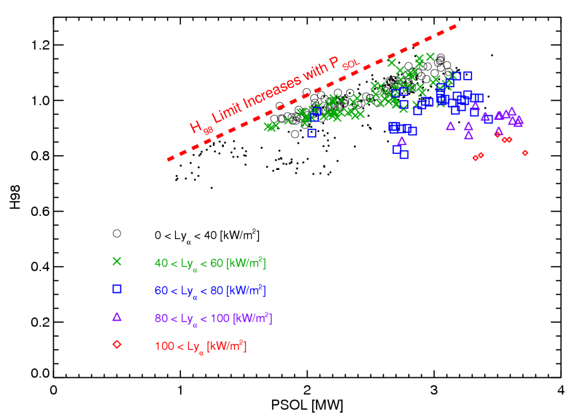

H98 Limit Increases with PSOL
H98
PSOL [MW]
0 < Lyα < 40 [kW/m2]
40 < Lyα < 60 [kW/m2]
60 < Lyα < 80 [kW/m2]
80 < Lyα < 100 [kW/m2]
100 < Lyα [kW/m2]

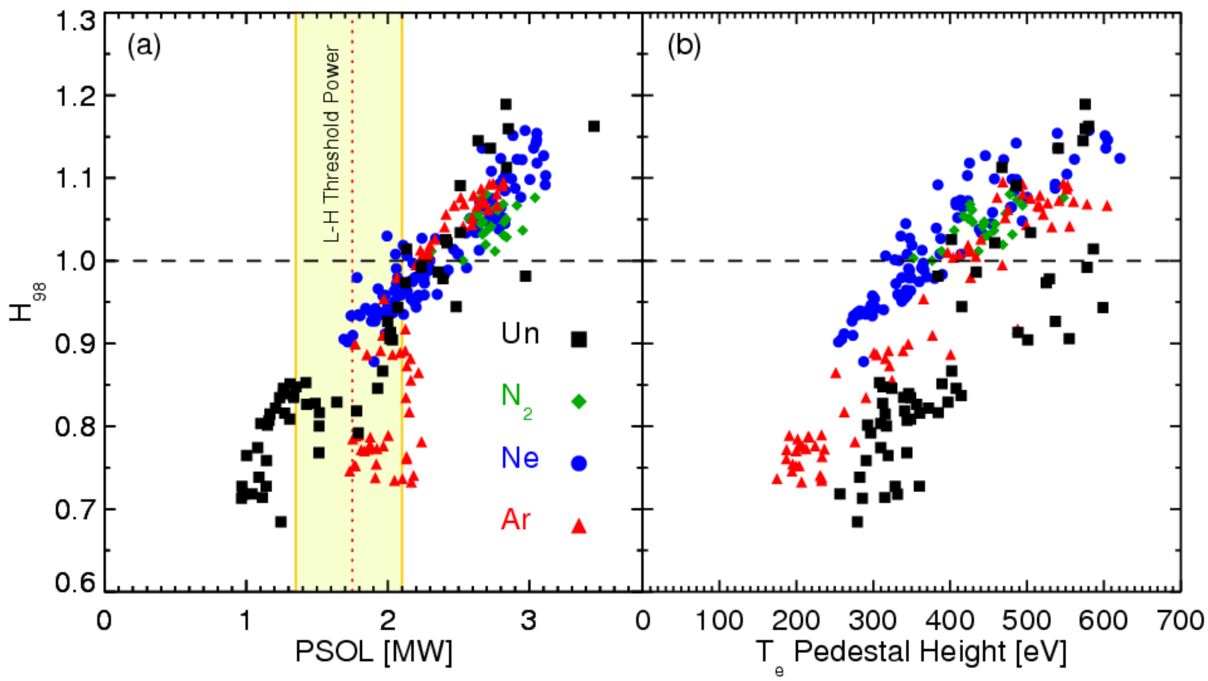
(a)
(b)
L-H Threshold Power
H98
PSOL [MW]
Te Pedestal Height [eV]
Un
N2
Ne
Ar

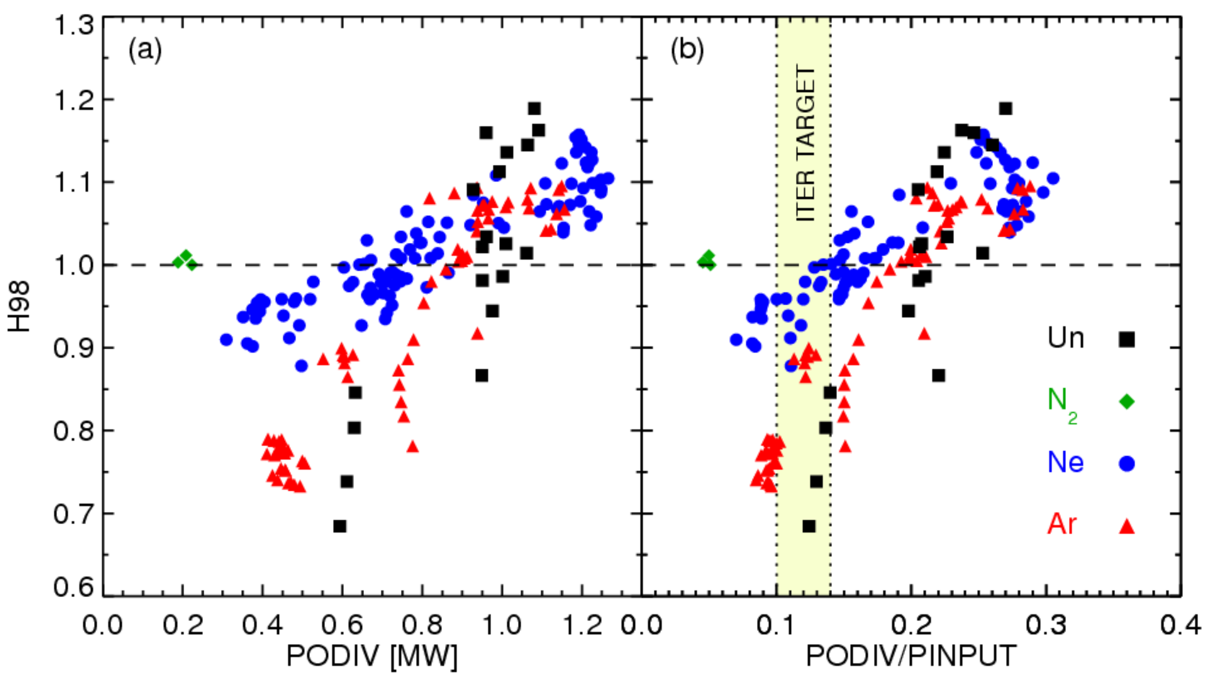
(a)
(b)
ITER TARGET
H98
PODIV [MW]
PODIV/PINPUT
Un
N2
Ne
Ar